Distorted magnetic island formation during slowing down to mode locking in helical plasmas

doi: 10.1088/1741-4326/aa6d26

Distorted magnetic island formation during slowing down to mode locking in helical plasmas

T. Tokuzawa[1], Y. Takemura[1,2], K.W. Watanabe[1], S. Sakakibara[1,2], Y. Narushima[1], H. Tsuchiya[1], Y. Nagayama[1,2], S. Inagaki[3], K. Ida[1,2], M. Yoshinuma[1,2], K. Tanaka[1], Y. Suzuki[1,2], I. Yamada[1], and the LHD Experiment Group[1]

[1]National Institute for Fusion Science, 322-6, Oroshi-cho, Toki-city, 509-5292, Japan

[2]SOKENDAI (The Graduate University for Advanced Study), 322-6 Oroshi, Toki-city, 509-5292, Japan

[3]Research Institute for Applied Mechanics, Kyushu University, 6-1 Kasuga-Koen, Kasuga-city, 816-8580, Japan

E-mail contact of main author: tokuzawa@nifs.ac.jp

Abstract. We report the first observation of the magnetic island formed before the appearance of the mode locking in helical plasma. New analysis and observation techniques applied to the ECE signal and poloidal flow in LHD experiments show the following results. (i) The magnetic island structure is present and rotating in the end of the rotating phase. (ii) The rotation speed of the island is not uniform in space and time. The rotation of the island changes significantly at the end of the rotating phase, and the deformation increases until the mode is locked.

1. Introduction

The study of the locked mode in some tokamak and RFP devices has been long history [1-4], because it is important in sometimes terminating discharges such as disruption. It is found that the instability of the tearing mode is a key physics and the formed magnetic island changes from the rotating phase to the locked phase. In the Large Helical Device (LHD), a rotating and/or non-rotating m/n=1/1 mode instability has been observed, and the former was identified as the resistive interchange mode [5-9]. In the case of non-rotating mode appeared discharge, the plasma show the following changes that at first the mode is oscillating and the magnetic fluctuation frequency shows a finite value (stationary rotating phase), then the frequency decreases and damps to zero (slowing down phase in rotating phase), finally the mode is locked and rapidly grows and leads a minor collapse (locked phase). It was found that the flattening of the electron temperature profile appears at the corresponding $\iota/2\pi$=1 surface and the rotation speed of the mode responds to the plasma flow. These phenomena have a similarity with the tokamak locked mode and for the moment we call these phenomena as locked mode like phenomena [10]. In the analogy of the tokamak locked tearing mode, the magnetic island existence has been implicated. The magnetic island itself has been studied and observed theoretically [11-13] and experimentally [14-16] in LHD. In the linear theory the interchange mode does not form the magnetic island, nonlinear interaction of the interchange mode and/or other physics might be affected in this phenomena. Therefore, the

observation of magnetic island structure during the precursor phase of this mode locking plasma is now a crucial issue.

In this paper, we report the first observation of the magnetic island formed before the appearance of the mode lock in the LHD plasma. From the point of view of identification of the island structure, the observations of spatial structure are important. These observations are presented in section 2.1. The interesting phenomena of the temporal behavior of the rotating magnetic island are described in 2.2 and 2.3. A summary are presented in section 3.

2. Experimental results

2.1. Identification of magnetic island structure

The LHD is a superconducting heliotron device with a major radius of 3.9 m and an averaged minor radius of 0.65 m [17]. In this experiment, the mode locking phenomena is observed under the condition that the magnetic axis position in the vacuum field is R_{ax} = 3.60 m, the magnetic field strength is B_t = 1.375 T, the helical coil pitch parameter γ = 1.1739, and the ratio of the quadrature field B_q = 100 %. The resonant magnetic perturbation coils (RMP coils) are used for cancellation of the error magnetic field. The magnetic field strength (1.375 T) is set for the availability of the electron cyclotron emission (ECE) measurements. The plasma is initiated and sustained by the electron cyclotron heating (ECH) and the neutral beam injection (NBI).

Figure 1 shows the typical time trace of the attending mode locking discharge. The plasma current and the line-averaged electron density gradually increase until t = 5.2 s. During the continuous NBI heating, the rotating m/n=1/1 magnetic fluctuation appears at around t = 4.5 s. The volume-averaged beta value $<\beta_{dia}>$ gradually decreases from t = 4.8 s and abruptly dropped at t = 5.2 s. The frequency of the magnetic fluctuation gradually decreases after around t = 4.8 s and then reaches almost zero at t = 5.2 s as shown in Fig. 1(g) (the end of the rotating phase). Just at this time the strong m/n=1/1 component of the radial magnetic field measured by the saddle loop array [18] rises rapidly as shown in Fig. 1(d) and the minor collapse occurs (locked phase).

At the beginning of the rotating phase, the clear indication of the magnetic island is obtained by ECE radiometer [19] as shown in Figs. 2(a) and (b). The rotating m/n=1/1 mode component included in the fluctuation amplitude and the phase difference of ECE intensity can be extracted by the digital filtering. The odd radial structure, which is an indication of the magnetic island structure, can be obtained. The flattened electron temperature T_e profile clearly appears as shown in Fig. 2(c). It is also found that the inverse position is nearly the same as the $\iota/2\pi$=1 surface. This structure is maintained during the rotating phase and the flattened region of the electron temperature profile increasingly expands until the locked phase. Therefore, we can find the magnetic island structure exists in the plasma before the appearance of the mode lock. This result means that the observation of the magnetic oscillation is caused by the rotating m/n=1/1 magnetic island.

Next, the rotating magnetic island phenomena in the rotating phase are expressed from the point of view of the flow velocity observation.

2.2. Observation of non-rigid rotating magnetic island

The magnetic island is well known to relate with the radial electric field and flow velocity. In the past LHD experiments with the enlarged static island by RMP coils, the measurement of the poloidal flow velocity was conducted [20]. This showed that the poloidal velocity is almost 0 km/s in the magnetic island and the large velocity shear is formed around the magnetic island. This result was obtained in the static magnetic island experiment. If the spontaneous rotation of magnetic island occurs, what will happen to the flow velocity? This time, we have tried to observe the flow velocity at the separated two toroidal positions by newly installed toroidally correlated microwave Doppler reflectometers [21, 22]. In addition, a poloidal flow against a toroidal flow is relatively important in this study.

Doppler reflectometer gives the temporal behaviour of perpendicular velocity $V_\perp$. The perpendicular velocity includes mainly the poloidal flow component rather than the radial component, and here we use this $V_\perp$ value as the indicator of poloidal flow velocity. In the rotating phase, $V_\perp$ at the toroidal position of ϕ= -72 degrees is oscillating at the same frequency as the magnetic fluctuation as shown in Fig. 1(e) and (f). Looking closely, the value of $V_\perp$ changes back and forth from around -10 to 0 km/s during the rotating phase as shown in Fig. 3(b). As mentioned above, the poloidal flow velocity is close to 0 km/s in the static magnetic island. Using this information, the observing two values change could be explained as follows. $V_\perp \sim 0$ km/s means that the O-point of the rotating magnetic island comes to the observation region. On the other hand, when the O-point of the magnetic island is absent in the observation point, the value of $V_\perp$ is the background flow velocity. Then, the signal oscillates between two values. In addition, Fig. 3(a) shows the radial component of m/n=1/1 magnetic flux. It should be noted that the toroidal location of the magnetic flux is different with both of reflectometers. The temporal change of radial profile of the $V_\perp$ are obtained by the multi channel Doppler reflectometer at the toroidal position of ϕ= +72 degrees shown in Fig. 4(b). Periodically $V_\perp \sim 0$ appears widely in the plasma edge region near the end of the rotating phase.

Regarding waveforms, two waveforms of time trace of $V_\perp$ shown in Figs. 3(b) and 4(a) are different. Each signal is observed at two toroidally separated locations as shown in Fig. 5(c). For the clarification of the waveform difference, the phase averaged calculation [23] is applied. Figure 5(b) shows the time evolutions of phase averaged $V_\perp$ in one oscillating period. Here, the horizontal axis represents one period of fluctuation at t = 5.10 – 5.15 s. The 'sojourn time' corresponding to the staying time of the O-point of the rotating magnetic island in the observation region (torus outer region) is different in the different toroidal locations. This suggests that the island structure is not steady because if the rotation is rigid and the shape is constant, the sojourn time must be the same at two positions. The sojourn time is considered to relate with the magnetic island width which is estimated by $\left(\Delta\Phi_{11}^{r}\right)^{0.5}\left(1-\cos\theta\right)$. Here, $\Delta\Phi_{11}^{r}$ is the m/n=1/1 component of the radial magnetic flux. Figure 6 shows the relationship between the sojourn time and the estimated island width. It is found that the sojourn time seems to be proportional to the width of the estimated magnetic island within the error bar and the difference of the two sojourn times is caused by the non-constant magnetic island structure in one oscillation period. Also, we found this structure changes with time. This is described in next section.

2.3. Observation of the changing structure of rotating magnetic island

Each sojourn time in one oscillation period is found to change not only in one oscillation period but also in long time duration. Figure 7 shows the temporal change of the phase averaged time evolution of $V_\perp$. The sojourn time of the signal at the position of ϕ= -72 degrees

enlarges. On the other hand, the sojourn time of the signal at the position of ϕ= +72 degrees becomes smaller. Also, the start timing of the sojourn time, which corresponds to the coming time of O–point, is delayed. This delay is presented by the phase difference between two $V_\perp$ measurements, and is shown in Fig. 1(h). At first, the phase difference is steady and equal to the separated toroidal angle of each diagnostics location. Then, after t = 5.12 s, the phase difference starts to change significantly.

This phenomenon might be possible to explain by the following two reasons. One is the shift of the start point in toroidal or poloidal space during the oscillation. The other is the change of the rotation speed in one oscillation period. Figure 8 shows the time evolution of the radial component of m/n=1/1 magnetic flux and the toroidal phase of O-point of the rotating magnetic island. Here, the toroidal phase is estimated from the correlation analysis of two saddle loop array signals. The start points of oscillation which is defined the timing of the minimum value of $\Delta\Phi_{11}^{r}$ every oscillation period are plotted by the green dots as shown in Fig. 8(b). The location is almost steady at around 0 radian. The temporal behaviour of the O-point moving toroidal location is plotted in Fig. 9. In this polar plot, one oscillation period at around t = 5.14 s is over plotted by the red square. The O-point location is rotating in a counter clockwise direction that is the electron diamagnetic direction. It is found that when the O-point locates at approximately 180 degrees, the amplitude of radial magnetic flux component $\Delta\Phi_{11}^{r}$ is large and almost constant. During the rotating phase, the amplitude becomes enlarged at around 0 degrees. At around ϕ= 180 degrees, the origin of the error field of LHD magnetic coils is located [24]. In this experiment, the operation is carried out under the cancelling error field condition. However, still the error field seems to be affected. Therefore, the shift of the start point should be omitted from the causes. For considering another candidate, the rotation speed is plotted with the amplitude of the radial magnetic flux component $\Delta\Phi_{11}^{r}$ in Fig. 10. They show the inverse relationship. When the rotation speed is high (low), the amplitude is small (large). Also, it is clearly found that there is hysteresis in one oscillation period and the shape of that hysteresis changes. This means that the rotation speed of the rotating magnetic island is not constant and it can be led to the phase change of the separate toroidal locations. In addition, this distortion of the rotation structure becomes large just before the locked phase, and finally it leads to the damping of the rotation velocity and the minor collapse.

3. Summary

This study found that for the stability of high performance plasma: (1) that the magnetic island structure is present in the mode locking discharge in helical plasma; (2) and that the island rotation speed is not toroidally uniform during the rotating phase. The non-uniformity increases until the mode is locked.

These observation results are quite similar with the tokamak locked mode observations. It will open the way to understand physical mechanics of locked mode in toroidal plasma which are not only helicals but also tokamaks. In this sense, the study of the reason why and what is the origin of the start of the rotating phase is important and must be understood in the future.

Acknowledgements

One of the authors (T.T.) wishes to thank Profs. K. Itoh, S-I. Itoh, T. Estrada, and C. Hidalgo for useful discussion. This work was partially supported in part by KAKENHI (Nos.

26630474 and 25289342), by a budgetary Grant-in-Aid of NIFS LHD project under the auspices of the NIFS Collaboration Research program (NIFS16ULPP027) and of the RIAM of Kyushu University. Also, this work was partially supported by Japan / U.S. Cooperation in Fusion Research and Development.

References

[1] Nave M.F.F. and Wesson J.A. 1990 *Nucl. Fusion* **30** 2575

[2] Morris A. W., *et al.* 1990 *Phys. Rev. Lett.* **64** 1254

[3] Zohm H. *et al.*, 1990 *Europhys. Lett.*, **11** (8) 745

[4] Fitzpatrick R. 1994 *Phys. Plasmas* **1** 3308

[5] Sakakibara S., *et al.* 2006 *Fusion Sci. Technol.* **50** 177

[6] Isayama A., *et al.* 2006 *Plasma Phys. Control. Fusion* **48** L45

[7] Watanabe K. Y., *et al.*2011 *Phys. Plasmas* **18** 056119

[8] Takemura Y., *et al.* 2013 *Plasma Fusion Res.* **8** 1402123

[9] Sakakibara S., *et al.* 2015 *Nucl. Fusion* **55** 083020

[10] Takemura Y., *et al.* 2012 *Nucl. Fusion* **52** 102001

[11] Nishimura S. *et al.* 2010 *Plasma Fusion Res.* **5** 040

[12] Nishimura S. *et al.* 2012 *Phys. Plasmas* **19** 122510

[13] Hegna C. C., 2012 *Phys. Plasmas* **19** 056101

[14] Ohyabu N., *et al.* 2002 *Phys. Rev. Lett.* **88** 055005

[15] Narushima Y., *et al.* 2008 *Nucl. Fusion* **48** 075010

[16] Narushima Y., *et al.* 2015 *Nucl. Fusion* **55** 073004

[17] Iiyoshi A., *et al.* 1999 *Nucl. Fusion* **39** 1245

[18] Sakakibara S., *et al.* 2010 *Fusion Sci. Technol.* **58** 471

[19] Nagayama Y., *et al.* 1999 *Rev. Sci. Instrum.* **70** 1021

[20] Ida K., *et al.* 2002 *Phys. Rev. Lett.* **88** 015002

[21] Tokuzawa T., *et al.* 2012 *Rev. Sci. Instrum.* **83** 10E322

[22] Tokuzawa T., *et al.* 2014 *Plasma Fusion Res.* **9** 1402149

[23] Cala C. E., *et al.* 2006 *Experiments in Fluids* **40** 267

[24] Sakakibara S., *et al.* 2013 *Nucl. Fusion* **53** 043010.

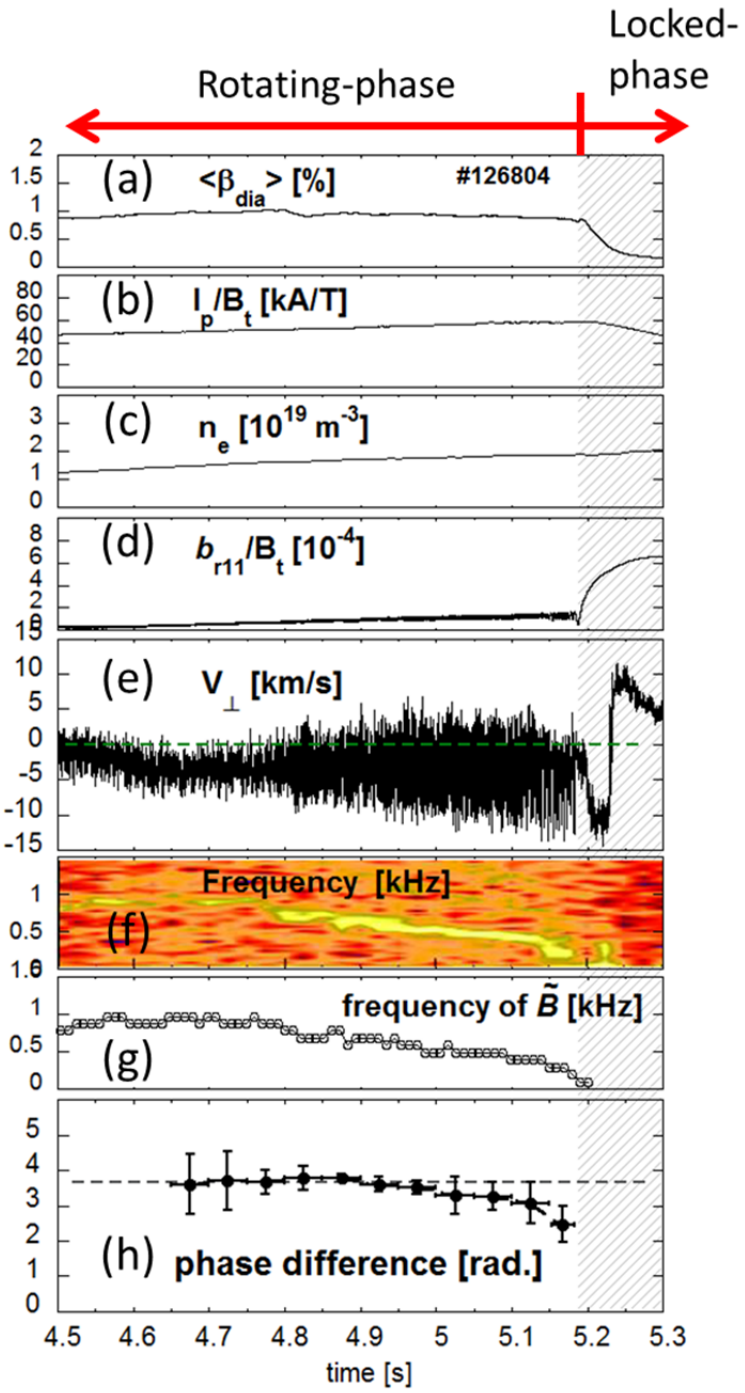

Fig. 1 Time evolutions of (a) volume-averaged β, (b) plasma current normalized to the toroidal field, (c) line-averaged electron density, (d) m/n=1/1 component of the radial magnetic field, (e) perpendicular velocity $V_\perp$ around r_{eff}/a_{99}=0.9, (f) frequency spectrogram of $V_\perp$, (g) frequency of m/n=1/1 magnetic fluctuation component, and (h) toroidal phase difference of $V_\perp$ oscillation component. Here, the locked-phase is shown by the hatching.

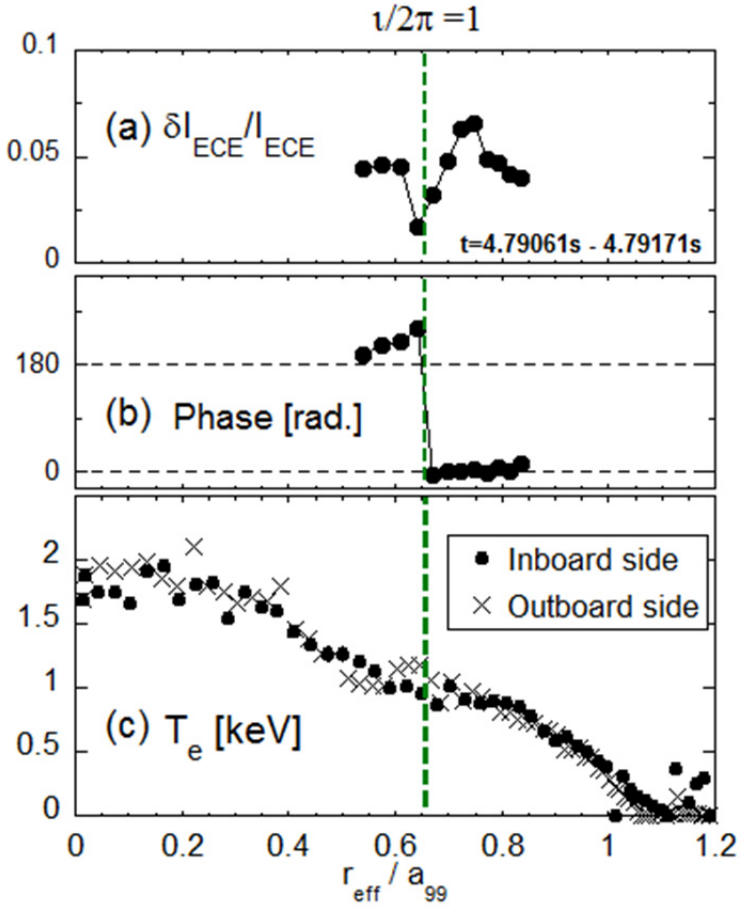

Fig. 2 Radial profiles of (a) fluctuation amplitude of m/n = 1/1 component of ECE intensity, (b) the phase difference, and (c) the flattened electron temperature measured by the Thomson scattering method at t =4.8 s.

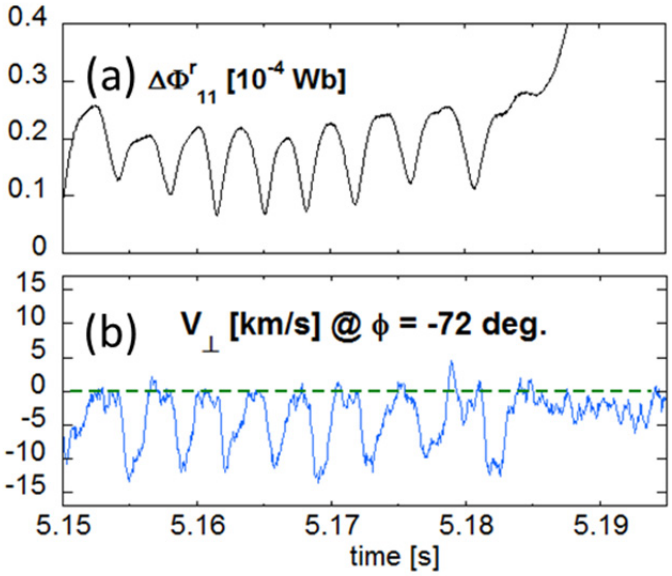

Fig. 3 Expanding view of the rotating phase oscillation just before the Locked-phase. The temporal change of (a) m/n=1/1 component of the radial magnetic flux and (b) the perpendicular velocity at the toroidal angle of ϕ = - 72 degrees.

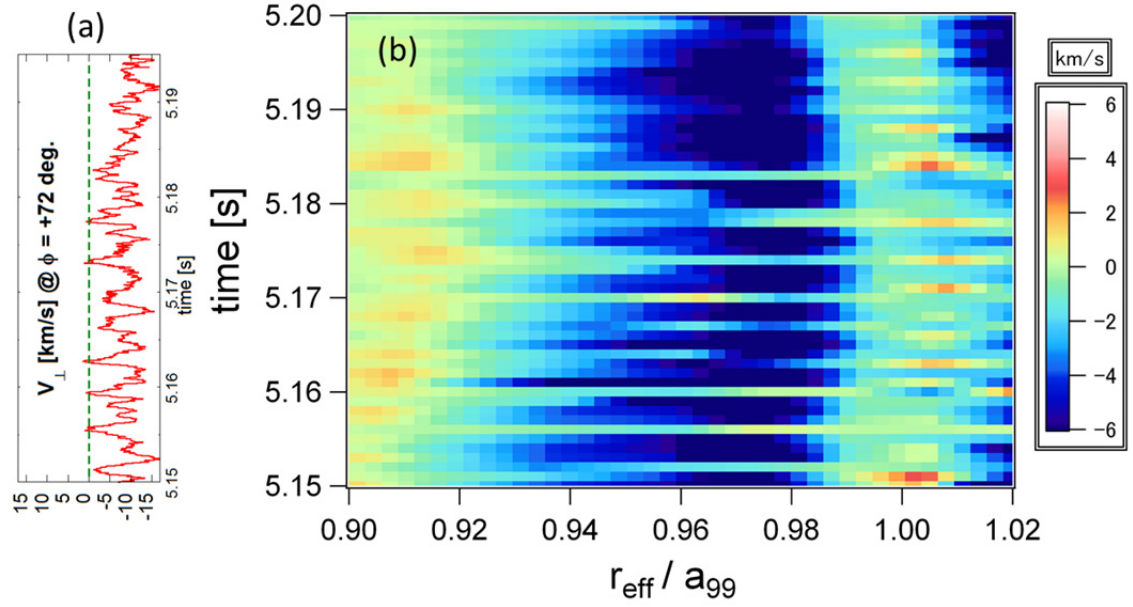

Fig. 4 (a) Time evolution of the perpendicular velocity $V_\perp$ at the toroidal angle of ϕ = + 72 degrees and r_{eff}/a_{99}=0.97, and (b) the spatio-temporal behavior of $V_\perp$ in the plasma edge region.

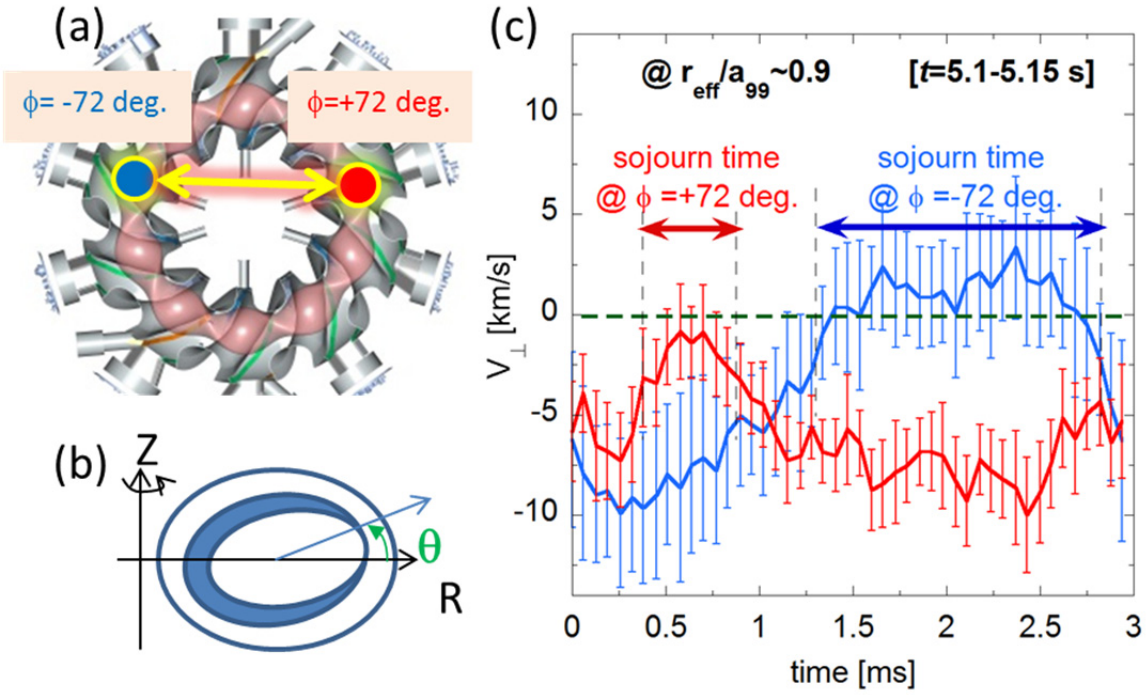

Fig. 5. (a) Schematic view of two toroidal observation locations of the toroidal angle ϕ = - 72 (blue) and +72 (red) degrees. (b) Schematic view of magnetic island. Here, θ is defined by the poloidal rotating angle from the horizontal axis. (c) Phase averaged time evolutions of $V_\perp$ with one-period of the fluctuation observed at two toroidal locations. Here, 19 ensembles are averaged according to the specific phase of m/n=1/1 component. The sojourn time in O-point is considered to be indicated by $V_\perp \sim 0$.

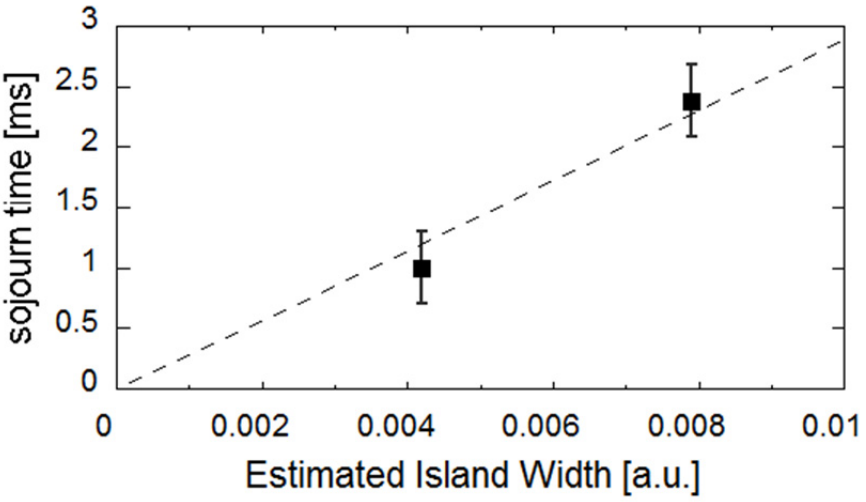

Fig. 6. Sojourn time as a function of the estimated island width.

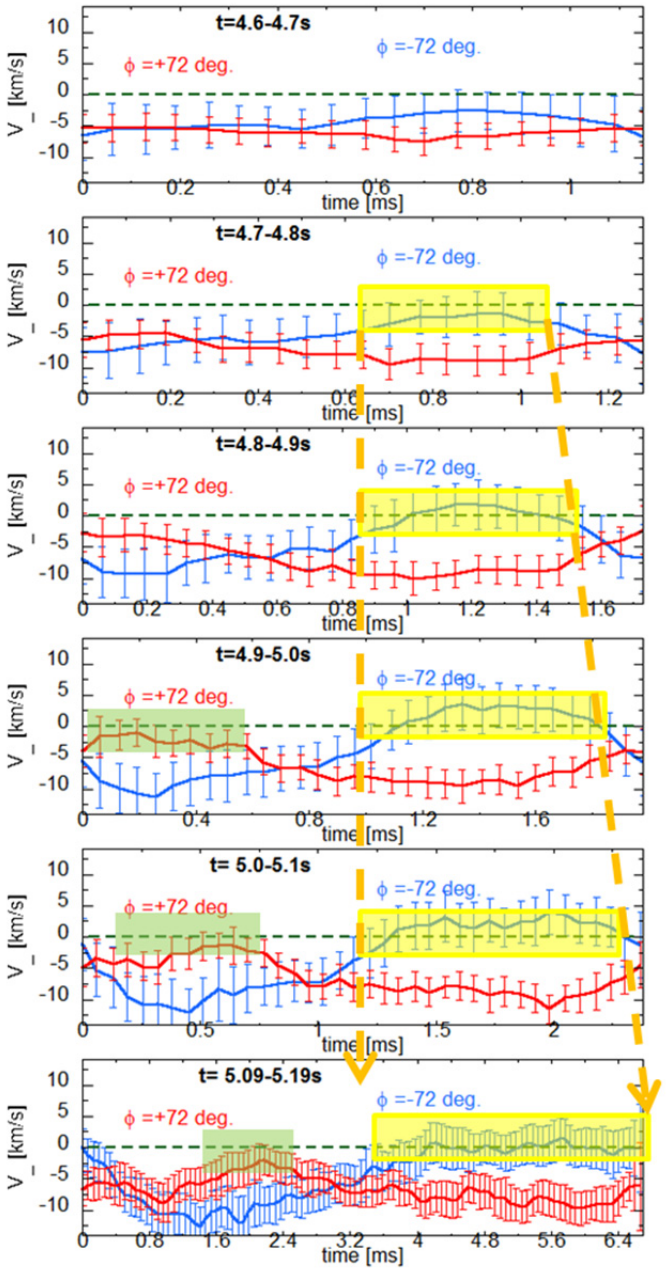

Fig. 7. From top to bottom, temporal changes of each phase averaged time evolutions of $V_{\perp}$ with one-period of the fluctuation observed at two toroidal locations of the toroidal angle ϕ = - 72 (blue) and +72 (red) degrees are shown. The estimated sojourn time of the two locations is indicated by the colored boxes.

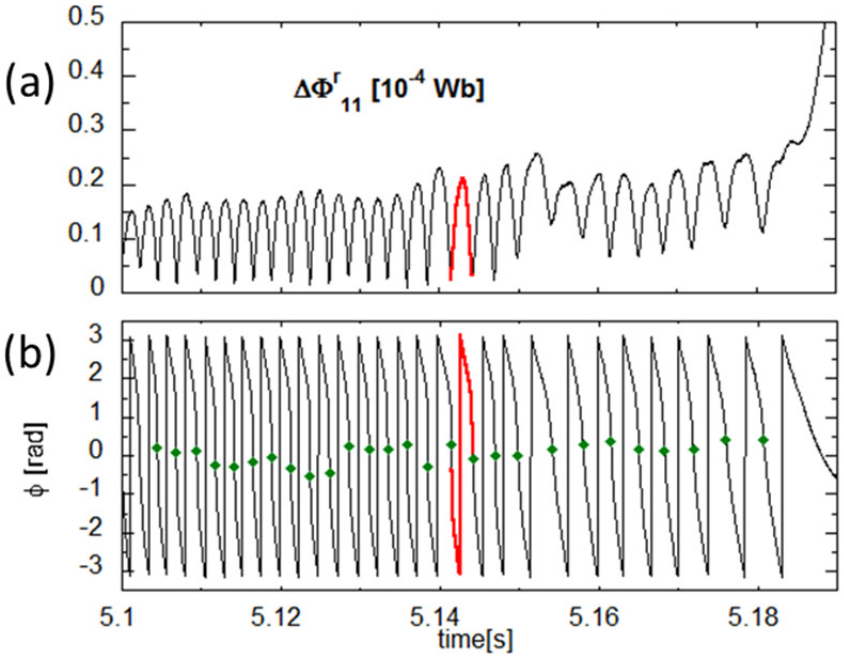

Fig. 8. Time evolution of the m/n=1/1 component of (a) the radial magnetic flux and (b) the toroidal phase of O-point. The start timings of the oscillation period are indicated by the green dots.

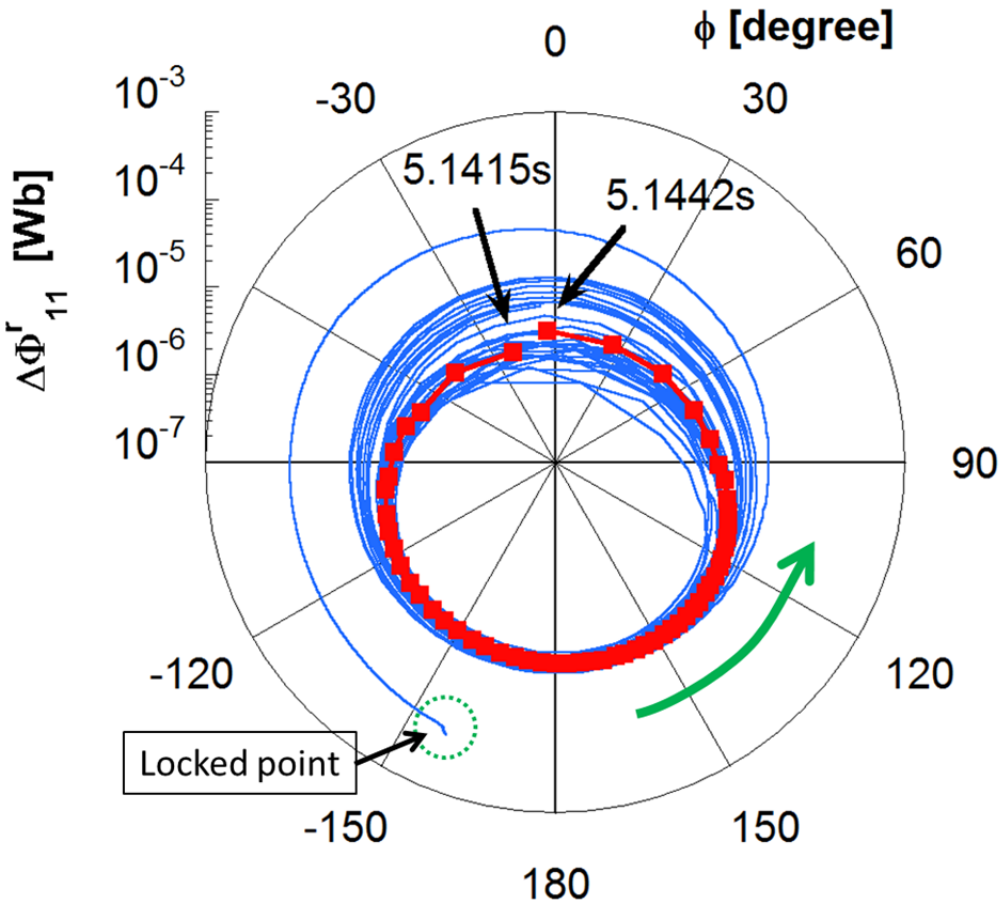

Fig. 9. Time evolution of the radial component of the m/n=1/1 magnetic flux as a function of toroidal angle during t= 5.1 – 5.19 s. A typical period which is indicated in Fig. 8 is over-plotted by red square and line.

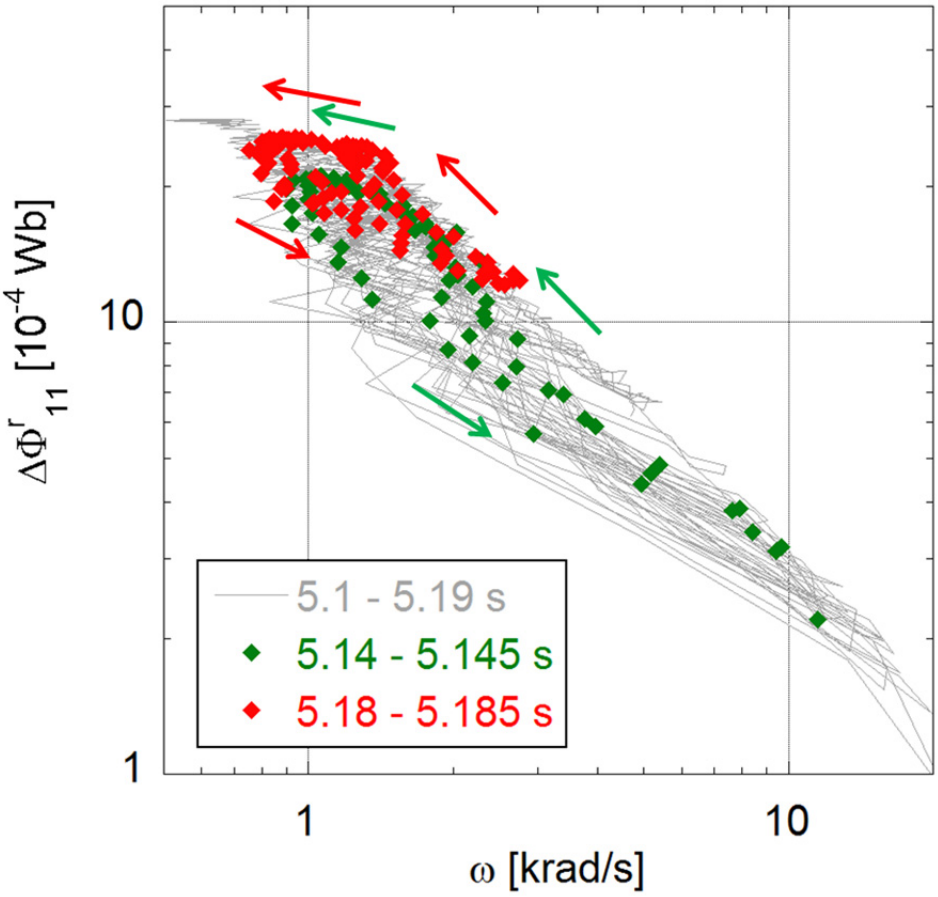

Fig. 10. Relationship between the rotation speed and the radial component of the m/n=1/1 magnetic flux. Two time slices are over-plotted by green and red diamonds.